Random-Phase-Approximation Dielectric Function of α-Sn in the Far Infrared*

J. G. Broerman
McDonnell Douglas Research Laboratories, McDonnell Douglas Corporation, St. Louis, Missouri 63166

The frequency-dependent random-phase-approximation (RPA) dielectric function of a symmetry-induced zero-gap semiconductor is examined in the far infrared. Expressions are derived for the temperature, wavelength, and impurity-concentration dependence in the degenerate and nondegenerate limits. It is shown that, at absolute zero, the real part of the dielectric function has a logarithmic singularity at a frequency corresponding to excitations to the Fermi surface. This singularity is removed by temperature and lifetime broadening. Numerical calculations are presented for cases of intermediate degeneracy in α-Sn at a number of impurity concentrations, temperatures, and lifetimes. It is shown that strong temperature dependences exist at liquid-helium temperatures and below. A recent experiment on the temperature dependence of the reflectivity minimum is analyzed and shown to be, with the exception of one low-temperature point, in excellent agreement with the theory. A value of 19 is determined for the background dielectric constant ϵ_0. Although the anomalous low-temperature datum can be quantitatively accounted for by small errors introduced by sample inhomogeneity into the Hall measurement of the carrier concentration, it is pointed out that the value of ϵ_0 inferred from this point yields electron mobilities in excellent agreement with experiment in the one-band region.

I. INTRODUCTION

Gray tin (α-Sn) is one of a family of materials of the diamond or zinc-blende structure whose highest-lying valence-band edge is degenerate with the lowest-lying conduction-band edge by reasons of symmetry.[1] If the dielectric function of this structure were well behaved, one would expect a collapse at low temperatures into a ground state of coherent bound electron-hole pairs.[2-5] However, it has been shown that the random-phase-approximation (RPA) static dielectric function of the pure material has a $1/q$ singularity at absolute zero[2-5] and a $T^{-1/2}$ temperature dependence[6] which radically reduce the electron-hole interaction. Whether or not this would prevent the transition to the excitonic phase is open to conjecture. However, it would certainly reduce the transition temperature, if it exists, to a very low value.

The attempt to establish the existence of this singularity in the dielectric function through its effect on some observable property[7-15] of these materials has attracted considerable interest. The situation at present is quite unclear. The ionized-impurity-limited mobility[7-14] and the near-infrared dielectric constant[15] have been examined. A term proportional to $\lambda^{1/2}$ was predicted[15] for the real part of the dielectric constant, but no deviation from the classical Drude form could be detected in the experimental data[16] for α-Sn. The ionized-impurity-limited mobility, as calculated[11,13] with the RPA dielectric function, should show anomalously large values at low impurity concentrations because of a low-impurity-concentration enhancement[7] in the static dielectric constant. However, the experimental values[17,18] for α-Sn are about $\frac{1}{3}$ of those predicted[11,13] in the RPA, but are in good agreement with a calculation[9] using the observed[16] concentration-independent background dielectric constant. On the other hand, the values predicted[12] using the RPA dielectric function are in good agreement with experiment in HgSe[19,20] and HgTe.[21] It has been suggested,[14] on the basis of the anomalous Γ_8^+-electron mobility observed[18] in the two-band (Γ_8^+ and L_6^+) region of impurity conduction, that the anomalously low mobility of α-Sn is due to scattering from neutral defects.

A calculation of the dielectric function in the far infrared is important for two reasons. First, the enhancement of the dielectric function is largest in this region. We will show that the dielectric function contains structure at low temperatures which should be experimentally observable, as well as temperature and wavelength dependences which we believe have been observed in a recent measurement[22] of the temperature dependence of the reflectivity minimum. Second, such an analysis is necessary to obtain a reliable value for the background dielectric constant which enters the mobility calculation.

II. GENERAL FORMULATION

The frequency- and momentum-transfer-dependent dielectric function in the RPA is given by[23-25]

$$\epsilon(\omega, q) = 1 - \frac{4\pi e^2}{q^2} \sum_{n,n',\vec{k}} \frac{|\langle \vec{k}, n | e^{-i\vec{q}\cdot\vec{r}} | \vec{k}+\vec{q}, n' \rangle|^2}{E_{\vec{k}+\vec{q},n'} - E_{\vec{k},n} - \hbar\omega - i\hbar/\tau_{n,n'}}$$

$$\times[f(E_{\vec{k}+\vec{q},n'})-f(E_{\vec{k},n})]\,, \quad (1)$$

where $\tau_{nn'}$ is a lifetime associated with the states involved and $f(E_{\vec{k},n})$ is the Fermi-Dirac distribution function. We define

$$\epsilon(\omega)=\lim_{q\to 0}\epsilon(\omega,q)\,, \quad (2)$$

and separate this into inter- and intraband parts

$$\epsilon(\omega)=\epsilon^{\text{inter}}(\omega)+\epsilon^{\text{intra}}(\omega)\,, \quad (3)$$

where

$$\epsilon^{\text{intra}}(\omega)=-\lim_{q\to 0}\frac{4\pi e^2}{q^2}\sum_{n,\vec{k}}\frac{|\langle\vec{k},n|e^{-i\vec{q}\cdot\vec{r}}|\vec{k}+\vec{q},n\rangle|^2}{E_{\vec{k}+\vec{q},n}-E_{\vec{k},n}-\hbar\omega-i\hbar/\tau_n}[f(E_{\vec{k}+\vec{q},n})-f(E_{\vec{k},n})]=\epsilon_1^{\text{intra}}+i\epsilon_2^{\text{intra}} \quad (4)$$

and

$$\epsilon^{\text{inter}}(\omega)=1-\lim_{q\to 0}\frac{4\pi e^2}{q^2}\sum_{\substack{n,n',\vec{k}\\ n\neq n'}}\frac{|\langle\vec{k},n|e^{-i\vec{q}\cdot\vec{r}}|\vec{k}+\vec{q},n'\rangle|^2}{E_{\vec{k}+\vec{q},n'}-E_{\vec{k},n}-\hbar\omega-i\hbar/\tau_{nn'}}[f(E_{\vec{k}+\vec{q},n'})-f(E_{\vec{k},n})]\,. \quad (5)$$

The intraband parts are given by the usual expressions:

$$\epsilon_1^{\text{intra}}(\omega)=-\frac{4\pi e^2}{m_0}\sum_i\frac{n_i}{\mu_i^*}\frac{1}{\omega^2+1/\tau_i^2}\,, \quad (6)$$

$$\epsilon_2^{\text{intra}}(\omega)=\frac{4\pi e^2}{m_0}\sum_i\frac{n_i}{\mu_i^*}\frac{1}{\omega\tau_i}\frac{1}{(\omega^2+1/\tau_i^2)}\,, \quad (7)$$

where m_0 is the mass of the free electron, μ_i^* is the optical effective-mass ratio of the ith band, and n_i is the carrier population of the ith band. We further separate $\epsilon^{\text{inter}}(\omega)$ into a contribution from the Γ_8^+ conduction and valence bands and a background part ϵ_0 from all other bands. We assume that all other bands are sufficiently remote from the Γ_8^+ bands that ϵ_0 is independent of frequency and carrier concentration and that its imaginary part is zero:

$$\epsilon^{\text{inter}}(\omega)=\epsilon_1^{\text{inter}}(\omega)+i\epsilon_2^{\text{inter}}(\omega)\,,$$

$$\epsilon_1^{\text{inter}}(\omega)=\epsilon_0-\frac{e^2}{\pi^2}\lim_{q\to 0}\frac{1}{q^2}\,\text{Re}[I(\omega,q)]\,, \quad (8)$$

$$\epsilon_2^{\text{inter}}(\omega)=-\frac{e^2}{\pi^2}\lim_{q\to 0}\frac{1}{q^2}\,\text{Im}[I(\omega,q)]\,, \quad (9)$$

$$I(\omega,q)=\int d^3k\left\{\left(\frac{|\langle\vec{k},v|e^{-i\vec{q}\cdot\vec{r}}|\vec{k}+\vec{q},c\rangle|^2}{E_{\vec{k}+\vec{q},c}-E_{\vec{k},v}-\hbar\omega-i\hbar/\tau_s}\times[f(E_{\vec{k}+\vec{q},c})-f(E_{\vec{k},v})]+\frac{|\langle\vec{k},c|e^{-i\vec{q}\cdot\vec{r}}|\vec{k}+\vec{q},v\rangle|^2}{E_{\vec{k}+\vec{q},v}-E_{\vec{k},c}-\hbar\omega-i\hbar/\tau_s}\times[f(E_{\vec{k}+\vec{q},v})-f(E_{\vec{k},c})]\right)\right\}. \quad (10)$$

Using $\vec{k}\cdot\vec{p}$ theory, the matrix element between the conduction and valence bands can be shown[2,11] to be

$$|\langle\vec{k},c|e^{-i\vec{q}\cdot\vec{r}}|\vec{k}+\vec{q},v\rangle|^2=\frac{3}{4}\frac{q^2\sin^2\alpha}{k^2+q^2+2kq\cos\alpha}\,, \quad (11)$$

where α is the angle between $\vec{k}$ and $\vec{q}$. With this result, the angular integration in (10) can be performed, the limit taken, and the result converted to an energy integral. This yields

$$\epsilon_1^{\text{inter}}(\omega)=\epsilon_0+\frac{\sqrt{2}\,e^2}{\pi\hbar}\frac{(\mu_c m_0)^{1/2}}{(1+\gamma)}\,\text{Re}[J(\omega)]\,, \quad (12)$$

$$\epsilon_2^{\text{inter}}(\omega)=\frac{\sqrt{2}\,e^2}{\pi\hbar}\frac{(\mu_c m_0)^{1/2}}{(1+\gamma)}\,\text{Im}[J(\omega)]\,, \quad (13)$$

where

$$J(\omega)=\int_0^\infty\frac{G(E)}{E^{1/2}}\left(\frac{1}{E-\hbar(\omega+i/\tau_s)/(1+\gamma)}+\frac{1}{E+\hbar(\omega+i/\tau_s)/(1+\gamma)}\right)dE\,, \quad (14)$$

$$G(E)=f(-\gamma E)-f(E)\,, \quad (15)$$

$$\gamma=\mu_c/\mu_v\,, \quad (16)$$

and μ_c and μ_v are the conduction- and valence-band density-of-states effective-mass ratios, respectively. At nonzero temperatures it is convenient to recast this in the form

$$\epsilon_1^{\text{inter}}(\omega)=\epsilon_0+\frac{\sqrt{2}\,e^2}{\pi\hbar}\frac{(\mu_c m_0)^{1/2}}{(1+\gamma)}\frac{1}{(k_BT)^{1/2}}\,\text{Re}[J'(\omega)]\,, \quad (17)$$

$$\epsilon_2^{\text{inter}}(\omega)=\frac{\sqrt{2}\,e^2}{\pi\hbar}\frac{(\mu_c m_0)^{1/2}}{(1+\gamma)}\frac{1}{(k_BT)^{1/2}}\,\text{Im}[J'(\omega)]\,, \quad (18)$$

$$J'(\omega)=\int_0^\infty\frac{G(y;z,\gamma)}{y^{1/2}}\left(\frac{1}{y-x-ix_s}+\frac{1}{y+x+ix_s}\right)dy\,, \quad (19)$$

where

$$G(y;z,\gamma)=\frac{e^{y-z}(1-e^{-(1+\gamma)y})}{(e^{-\gamma y-z}+1)(e^{y-z}+1)}\,, \quad (20)$$

$$z=E_F/k_BT\,, \quad (21)$$

$$x=\hbar\omega/(1+\gamma)k_BT\ , \tag{22}$$

$$x_s=T_s/[(1+\gamma)T]\ . \tag{23}$$

The quantity T_s, a scattering temperature which at low temperatures we assume to be of the same order of magnitude as the Dingle temperature, is defined by

$$T_s=\hbar/k_B\tau_S\ , \tag{24}$$

and E_F is the Fermi energy.

III. DEGENERATE INFINITE-LIFETIME LIMIT

For this case

$$1/\tau_s=0 \tag{25}$$

and

$$G(E)=\theta(E_F'-E)\ , \tag{26}$$

where

$$E_F'=\begin{cases} E_F\ , & E_F>0 \\ -E_F/\gamma\ , & E_F<0 \end{cases} \tag{27}$$

and θ is the step function

$$\theta(u)=\begin{cases} 0, & u>0 \\ 1, & u<0 \end{cases}\ . \tag{28}$$

The integral $J(\omega)$ can then be evaluated in closed form. The real and imaginary parts of the dielectric function are then found to be

$$\epsilon_1^{\text{inter}}(\omega)=\epsilon_0+\frac{2\sqrt{2}e^2}{\pi\hbar^{3/2}}\left(\frac{\mu_c m_0}{1+\gamma}\right)^{1/2} \times\frac{1}{\omega^{1/2}}\left\{\frac{\pi}{2}-\tan^{-1}\left(\frac{(1+\gamma)E_F'}{\hbar\omega}\right)^{1/2} +\frac{1}{2}\ln\left|\left[1+\left(\frac{(1+\gamma)E_F'}{\hbar\omega}\right)^{1/2}\right]\Big/\left[1-\left(\frac{(1+\gamma)E_F'}{\hbar\omega}\right)^{1/2}\right]\right|\right\}, \tag{29}$$

$$\epsilon_2^{\text{inter}}(\omega)=\frac{\sqrt{2}e^2}{\hbar}\left(\frac{\mu_c m_0}{1+\gamma}\right)^{1/2}\frac{\theta[(1+\gamma)E_F'-\hbar\omega]}{(\hbar\omega)^{1/2}}\ . \tag{30}$$

Thus, $\epsilon_1^{\text{inter}}(\omega)$ has a logarithmic singularity and $\epsilon_2^{\text{inter}}$ a finite discontinuity at $\hbar\omega=(1+\gamma)E_F'$. The zero-momentum-transfer singularity of the static dielectric function is simply moved to a higher frequency by the presence of impurity carriers. At large ω [i.e., $\hbar\omega\gg(1+\gamma)E_F'$], Eq. (29) yields the $\lambda^{1/2}$ dependence of Ref. 15, while at small ω [$\hbar\omega\ll(1+\gamma)E_F'$], it yields the static dielectric constant of Ref. 7.

This singularity in $\epsilon_1^{\text{inter}}(\omega)$ is removed by thermal and lifetime broadening. However, as we shall see in Secs. IV and V, a large strongly temperature-dependent enhancement should still remain at liquid-helium temperatures at the singular frequency.

It is interesting to speculate whether the singularity in $\epsilon_1^{\text{inter}}(\omega)$ has an observable effect on the lattice dynamics of the symmetry-induced zero-gap structures.

IV. THERMAL BROADENING

For this case we keep the restriction of infinite lifetime but relax the requirement of perfect degeneracy. Then Eqs. (17)–(19) reduce to

$$\epsilon_1^{\text{inter}}(\omega)=\epsilon_0+\frac{2\sqrt{2}}{\pi\hbar}\frac{(\mu_c m_0)^{1/2}}{(1+\gamma)}\frac{e^2}{(k_BT)^{1/2}} \times P\int_0^\infty\frac{y^{1/2}G(y;z,\gamma)}{y^2-x^2}\,dy \tag{31}$$

and

$$\epsilon_2^{\text{inter}}(\omega)=\frac{\sqrt{2}\,e^2(\mu_c m_0)^{1/2}}{\hbar(k_BT)^{1/2}(1+\gamma)}\frac{G(x;z,\gamma)}{x^{1/2}}\ . \tag{32}$$

In order to evaluate this principal-value integral we rewrite it as

$$P\int_0^\infty\frac{y^{1/2}G(y;z,\gamma)}{y^2-x^2}\,dy=F(x,z,\gamma) =R(x,z,\gamma;y_0)+P(x,z,\gamma;y_0)\ , \tag{33}$$

where

$$R(x,z,\gamma;y_0)=\int_0^{x-y_0}\frac{y^{1/2}G(y;z,\gamma)}{y^2-x^2}\,dy +\int_{x+y_0}^\infty\frac{y^{1/2}G(y;z,\gamma)}{y^2-x^2}\,dy\ , \tag{34}$$

$$P(x,z,\gamma;y_0)=P\int_{x-y_0}^{x+y_0}\frac{y^{1/2}G(y;z,\gamma)}{y^2-x^2}\,dy\ , \tag{35}$$

and y_0 is only restricted to be less than x. After a straightforward but tedious calculation, one obtains the following result for the principal part, $P(x,z,\gamma;y_0)$:

$$P(x,z,\gamma;y_0)=2[x^{1/2}G(x;z,\gamma)-2xC_1]\phi_0 +2\sum_{n=1}^{\infty}(C_{2n}-2xC_{2n+1})\phi_n\ , \tag{36}$$

where the ϕ_n are defined by the recursion relations

$$\phi_n=y_0^{2n-1}/(2n-1)+4x^2\phi_{n-1}\ , \tag{37}$$

with

$$\phi_0=-\frac{1}{4x}\ln\left|\frac{2x+y_0}{2x-y_0}\right|\ . \tag{38}$$

The C_n are defined by

$$C_n=G(x;z,\gamma)B_n+x^{1/2}A_n+\sum_{m=1}^{n-1}A_mB_{n-m}\ , \tag{39}$$

and the B_n are defined by the recursion relation

$$B_n = (3/2n-1)x^{-1}B_{n-1}\,, \tag{40}$$

with

$$B_0 = x^{1/2}\,. \tag{41}$$

The A_n are given by

$$A_n = \frac{1}{n!}\sum_{m=1}^{n} b_m^n \{(-\gamma)^n e^{-m(\gamma x+z)}[f(-\gamma x)]^{m+1} - e^{m(x-z)}[f(x)]^{m+1}\}\,, \tag{42}$$

where

$$f(u) = (e^{u-z}+1)^{-1}\,, \tag{43}$$

and the b_m^n are defined by the recursion relation

$$b_m^n = m[b_m^{n-1} - b_{m-1}^{n-1}]\,, \tag{44}$$

with the conditions

$$b_1^1 = -1\,, \tag{45}$$

$$b_m^n = 0\,, \quad m<1 \tag{46}$$

$$b_m^n = 0\,, \quad m>n\,. \tag{47}$$

Although this appears quite formidable, it is actually very simple to generate on a computer because of its formulation in terms of recursion relations. $R(x, z, \gamma; y_0)$ is integrated numerically, using easily generated analytic approximations in those ranges in which $G(y; z, \gamma)$ is approximately constant in y.

We can now examine the nondegenerate limit. For this case

$$n_e \sim n_h \gg Z_D N_D - Z_A N_A\,, \tag{48}$$

where n_e and n_h are the densities of electrons and holes, respectively, and $Z_D N_D - Z_A N_A$ is the net ionized-impurity concentration. Under these conditions, in a two-band model, z is given by the solution of the equation

$$F_{1/2}(-z)/F_{1/2}(z) = \gamma^{3/2}\,; \tag{49}$$

that is, z, and hence $F(x, z, \gamma)$, become independent of temperature. $F_{1/2}(z)$ is the Fermi function[26] of order $\frac{1}{2}$. Thus,

$$F(x, z, \gamma) = F(x, \gamma) \tag{50}$$

and

$$\epsilon_1^{\text{inter}}(\omega) = \epsilon_0 + \frac{2\sqrt{2}\,(\mu_c m_0)^{1/2}}{\pi\hbar(1+\gamma)}\frac{e^2}{(k_B T)^{1/2}}F(x, \gamma)\,. \tag{51}$$

Note that the approximate solution of Eq. (49) given by Eq. (10) of Ref. 6 is not very accurate in the range of interest of γ. This does not affect the results shown in Fig. 1 of Ref. 6 since an exact numerical solution of Eq. (49) of this paper was actually used in that calculation.

In Fig. 1 we show some numerical calculations of the universal function $F(x, \gamma)$ for a variety of values of γ. For small x, the function is approximately constant and equal to $F(\gamma)$ shown in Fig. 1 of Ref. 6. It goes through a slight maximum, which is much more pronounced for small γ, near $x=1$ and then assumes an $x^{-1/2}$ dependence, independent of γ.

It should be noted that this limit is not useful in the three-band region, that is, to not much above 120 K, in α-Sn. This is because the low-lying L_6^+ bands considerably perturb the solution of Eq. (49). In general, α-Sn demands a numerical solution of the equation

$$\frac{1}{2\pi^2}\left(\frac{2m_0 k_B T}{\hbar^2}\right)^{1/2}[\mu_c^{3/2}F_{1/2}(z) + 4\mu_1^{3/2}F_{1/2}(z - E_{g1}/k_B T) - \mu_v^{3/2}F_{1/2}(-z)]$$

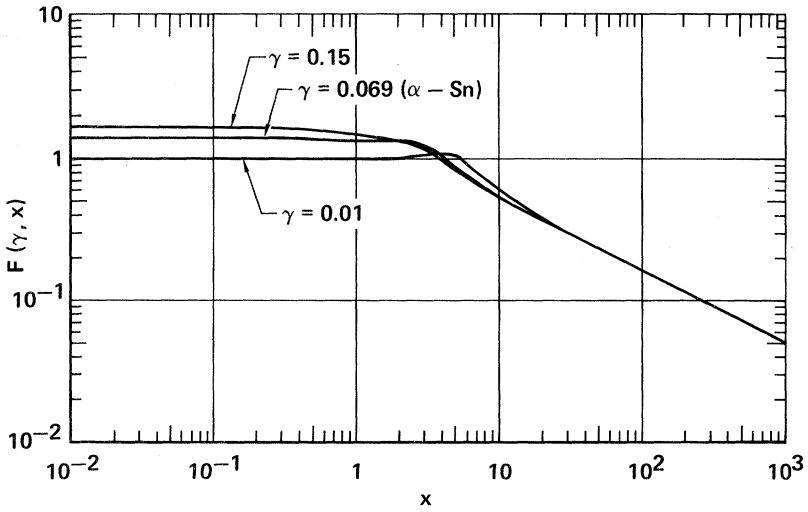

FIG. 1. The universal function $F(x, \gamma)$ for some relevant values of γ.

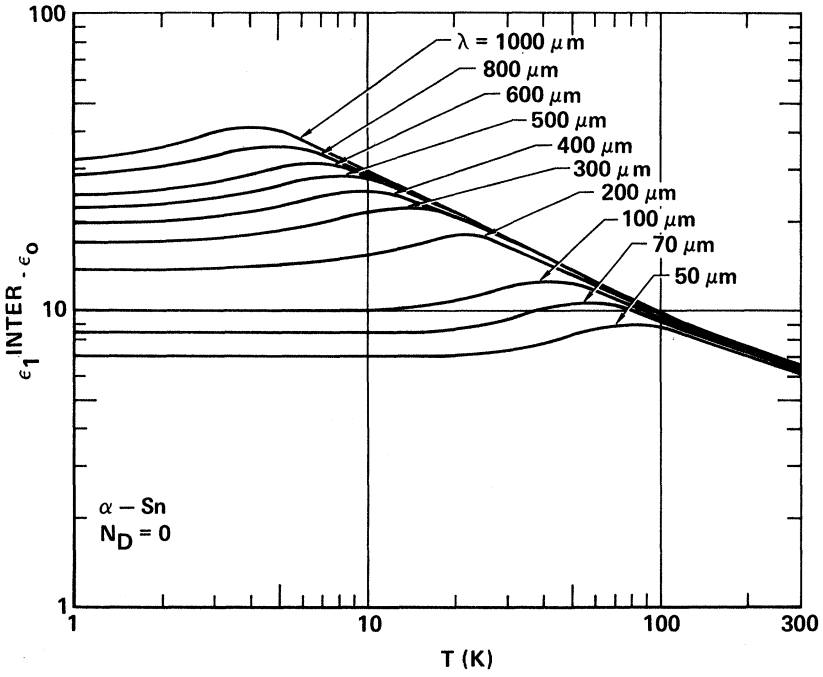

FIG. 2. The temperature dependence of $\epsilon_1^{\text{inter}}(\omega) - \epsilon_0$ at constant wavelength for pure α-Sn.

$$= Z_D N_D - Z_A N_A \,, \quad (52)$$

and no universal function, not explicitly dependent on temperature, can be constructed from $F(x, z, \gamma)$. E_{g1} is the $L_6^+ - \Gamma_8^+$ energy gap, and μ_1 is the density-of-states effective-mass ratio of each of the four nonequivalent L_6^+ minima. In Fig. 2 is shown a calculation of $\epsilon_1^{\text{inter}} - \epsilon_0$ as a function of temperature

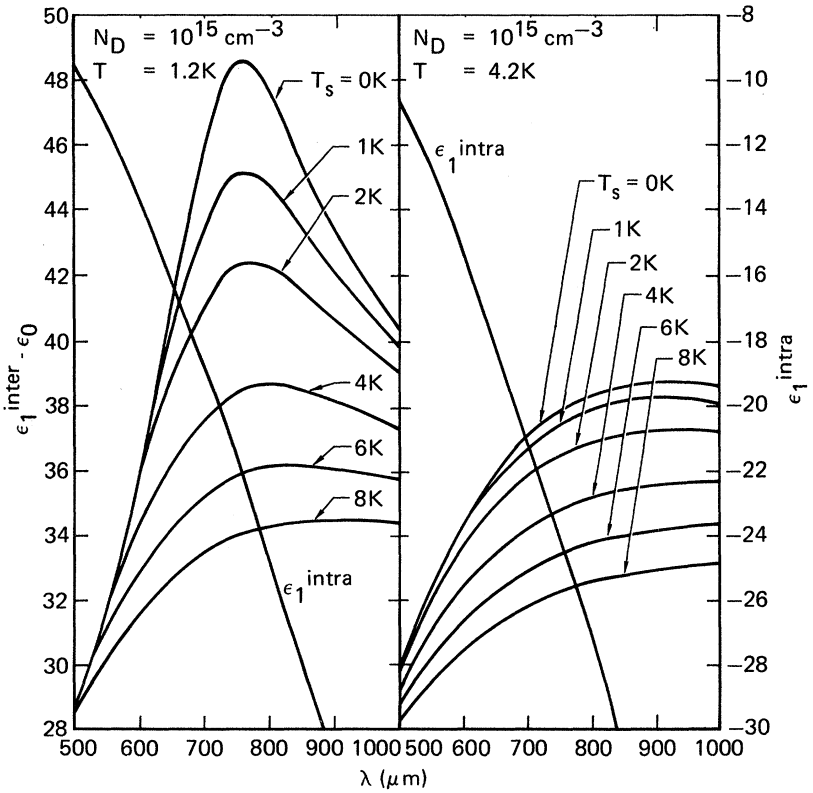

FIG. 3. $\epsilon_1^{\text{inter}}(\omega) - \epsilon_0$ in the region around the degenerate singularity of α-Sn for a donor concentration of 10^{15} cm^{-3} at two temperatures in the liquid-helium range and a number of values of the scattering temperature. The curves shown for $\epsilon_1^{\text{intra}}$ are for infinite lifetime.

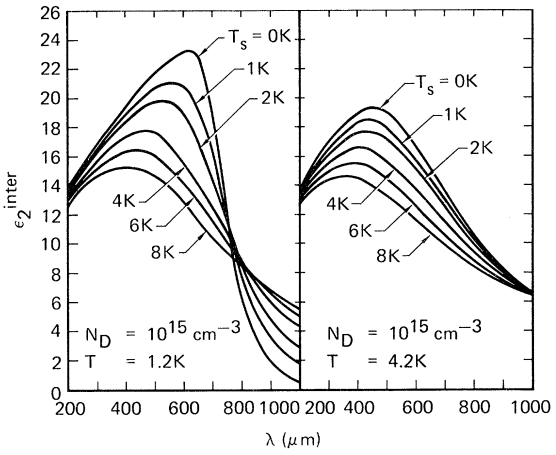

FIG. 4. $\epsilon_2^{\text{inter}}(\omega)$ in the region around the degenerate finite discontinuity of α-Sn for a donor concentration of 10^{15} cm^{-3} at two temperatures in the liquid-helium range and a number of values for scattering temperature.

at constant wavelength. We have used the parameters $\mu_c = 0.024$,[27] $\mu_v = 0.337$,[27] $\mu_1 = 0.17$,[18] $E_{g1} = 0.092$,[18] and $N_D = N_A = 0$. The curves are constant at low temperature, go through a small maximum, assume a $T^{-1/2}$ dependence, and then flatten at high temperatures because of the presence of the L_6^+ bands. The maximum is much more pronounced in materials with very small values of γ, such as the $Hg_{1-x}Cd_xTe$ system near the crossover composition.

The behavior of the real part of the dielectric constant of almost-degenerate samples near the singular point of the degenerate case is extremely important. In Figs. 3–8 are shown the real and imaginary parts of the dielectric function of α-Sn at two temperatures in the liquid-helium range in a wavelength region around the singular point for three carrier concentrations. These are the curves labeled $T_s = 0$. As can be seen, the structure remaining from the singularity is still quite sharp, and there are large temperature dependences even at liquid-helium temperatures. This structure should be easily observable at $N_D = 10^{17}$ cm^{-3} by an ellipsometric experiment like that of Ref. 16, provided sufficiently clean samples can be obtained. This analysis also indicates that Eq. (29) is accurate to within 1% outside the frequency range $(1+\gamma)E_F' - 3kT < \hbar\omega < (1+\gamma)E_F' + 3kT$ for n-type samples and $(1+\gamma)E_F' - 3kT/\gamma < \hbar\omega < (1+\gamma)E_F' + 3kT/\gamma$ for p-type samples. Thus it provides a convenient analytical expression for fitting experimental data at low temperatures. The modification to the near-degenerate case by lifetime broadening is discussed in Sec. V.

V. LIFETIME BROADENING

For this case we relax the restriction $1/\tau_s = 0$. The expression for the real and imaginary parts of the dielectric constant are then given by

$$\epsilon_1^{\text{inter}}(\omega) = \epsilon_0 + \frac{2\sqrt{2}}{\pi\hbar}\,\frac{(\mu_c m_0)^{1/2}}{(1+\gamma)}\,\frac{e^2}{(k_B T)^{1/2}}\,F_1(x, x_s)\,, \tag{53}$$

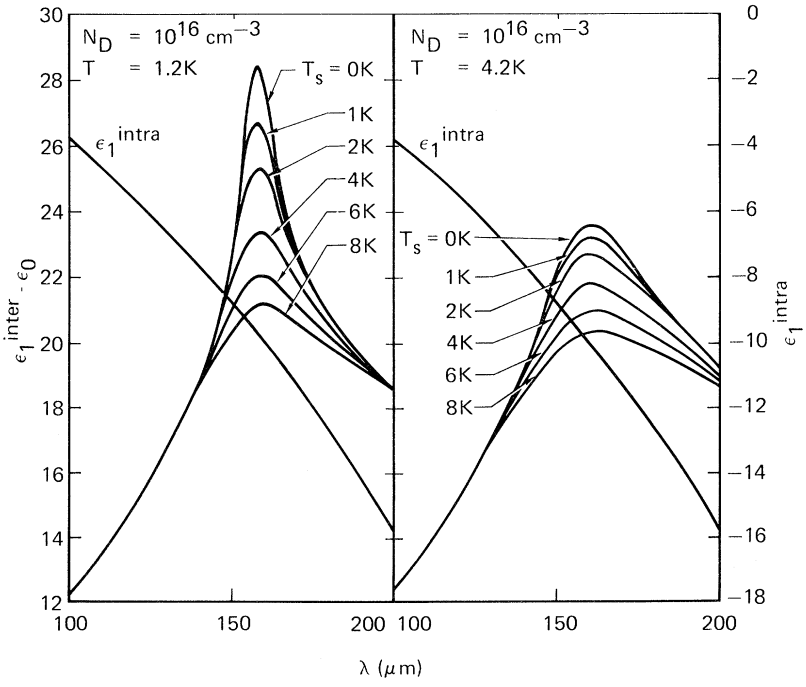

FIG. 5. $\epsilon_1^{\text{inter}}(\omega) - \epsilon_0$ in the region around the degenerate singularity of α-Sn for a donor concentration of 10^{16} cm^{-3} at two temperatures in the liquid-helium range and a number of values of the scattering temperature. The curves shown for $\epsilon_1^{\text{intra}}$ are for infinite lifetime.

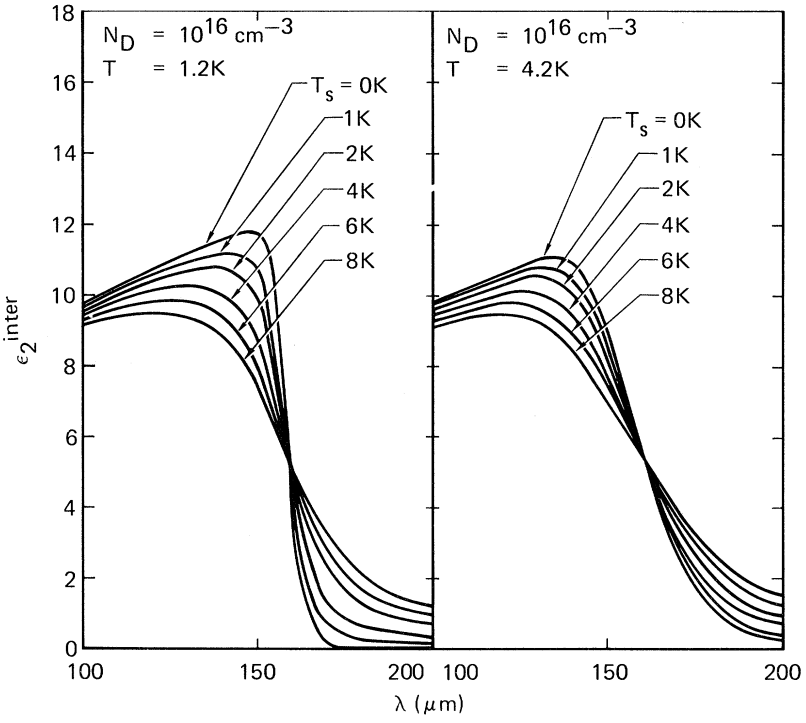

FIG. 6. $\epsilon_2^{\text{inter}}(\omega)$ in the region around the degenerate finite discontinuity of α-Sn for a donor concentration of 10^{16} cm^{-3} at two temperatures in the liquid-helium range and a number of values of the scattering temperature.

$$\epsilon_2^{\text{inter}}(\omega)=\frac{\sqrt{2}}{\hbar}\,\frac{(\mu_c m_0)^{1/2}}{(1+\gamma)}\,\frac{e^2}{(k_B T)^{1/2}}\,F_2(x,x_s)\,, \tag{54}$$

where

$$F_1(x,x_s)=\int_0^\infty \frac{G(y;z,\gamma)\,y^{1/2}\,(y^2-x^2+x_s^2)}{[(y-x)^2+x_s^2][(y+x)^2+x_s^2]}\,dy \tag{55}$$

and

$$F_2(x,x_s)=\frac{4}{\pi}\,xx_s\int_0^\infty \frac{y^{1/2}G(y;z,\gamma)}{[(y-x)^2+x_s^2][(y+x)^2+x_s^2]}\,dy\,. \tag{56}$$

We have calculated $\epsilon_1^{\text{inter}}$ and $\epsilon_2^{\text{inter}}$ in the neighborhood of the degenerate singularity for three concentrations of donors and a number of values of T_s. The results are shown in Figs. 3–8. As can be seen $\epsilon_2^{\text{inter}}$ is considerably more sensitive to T_s than $\epsilon_1^{\text{inter}}$. Thus, the results for $\epsilon_2^{\text{inter}}$ are probably not too reliable since we have assumed that T_s is independent of electron energy in a given sample. If $\epsilon_2^{\text{inter}}$ were measured experimentally, model-dependent calculations of T_s, which would yield information about the scattering mechanisms in these materials, would be quite worthwhile. For small values of T_s, the structure in $\epsilon_1^{\text{inter}}$ at the degenerate singular point should still be observable and have a strong temperature dependence.

If an experiment measuring $\epsilon_1^{\text{inter}}$ in a low-concentration n-type sample could be performed, it would yield considerable information about T_s at the Fermi surface. This is of some importance because, if large enough, it can affect the static dielectric constant, and hence the mobility. An approximate expression for this dependence is given by

$$\epsilon^{\text{inter}}(0)-\epsilon_0=\frac{2\sqrt{2}}{\pi\hbar}\,\frac{e^2(\mu_c m_0)^{1/2}}{(1+\gamma)}\,g(T_s,E_F)\,, \tag{57}$$

$$g(T_s,E_F)=\frac{1}{(2k_B T_s/(1+\gamma))^{1/2}}\times\left[\frac{1}{2}\ln\left(\frac{1+(2r)^{1/2}+r}{1-(2r)^{1/2}+r}\right)-\tan^{-1}\frac{(2r)^{1/2}}{r-1}\right]$$
$$\sim\frac{2}{E_F'^{1/2}}\left[1-\tfrac{1}{5}\,r^2+\tfrac{1}{9}r^4-\cdots\right], \tag{58}$$

and

$$r=k_B T_s/[(1+\gamma)E_F']\,. \tag{59}$$

This was derived under the condition $k_B T/|E_F| \ll 1$.

VI. TEMPERATURE DEPENDENCE OF REFLECTIVITY MINIMUM

Wagner and Ewald[22] have recently performed an experiment on the temperature dependence of the reflectivity minimum of α-Sn which has considerable relevance to the problem of the temperature, impurity concentration, and wavelength dependence of the dielectric function. However, before we examine this experiment we would like to discuss an older experiment on the dielectric function itself.

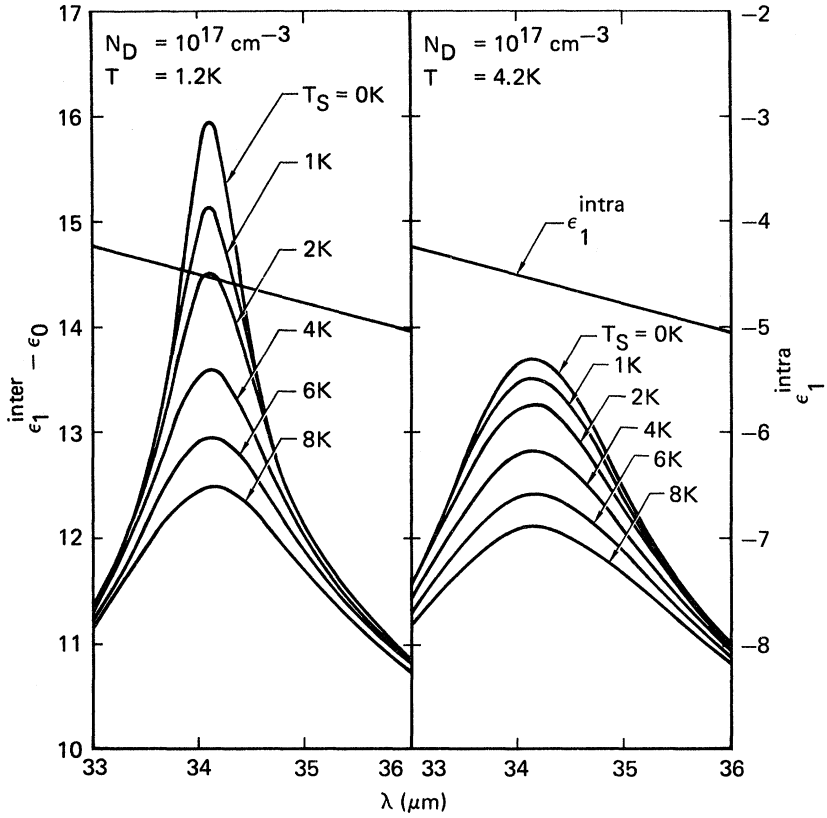

FIG. 7. $\epsilon_1^{\text{inter}}(\omega) - \epsilon_0$ in the region around the degenerate singularity of α-Sn for a donor concentration of 10^{17} cm^{-3} at two temperatures in the liquid-helium range and a number of values of the scattering temperature. The curves shown for $\epsilon_1^{\text{intra}}$ are for infinite lifetime.

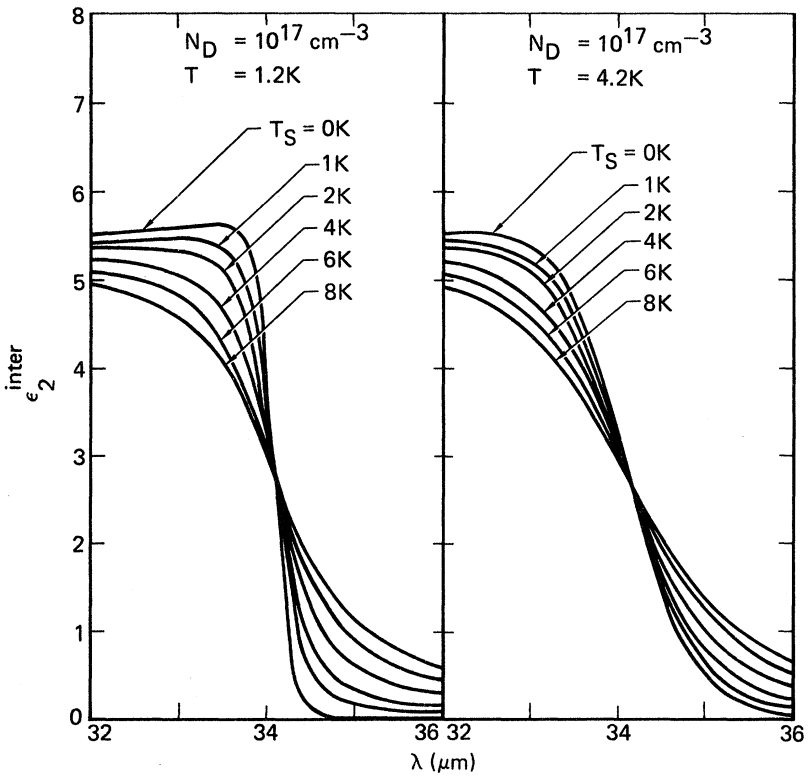

FIG. 8. $\epsilon_2^{\text{inter}}(\omega)$ in the region around the degenerate finite discontinuity of α-Sn for a donor concentration of 10^{17} cm^{-3} at two temperatures in the liquid-helium range and a number of values of the scattering temperature.

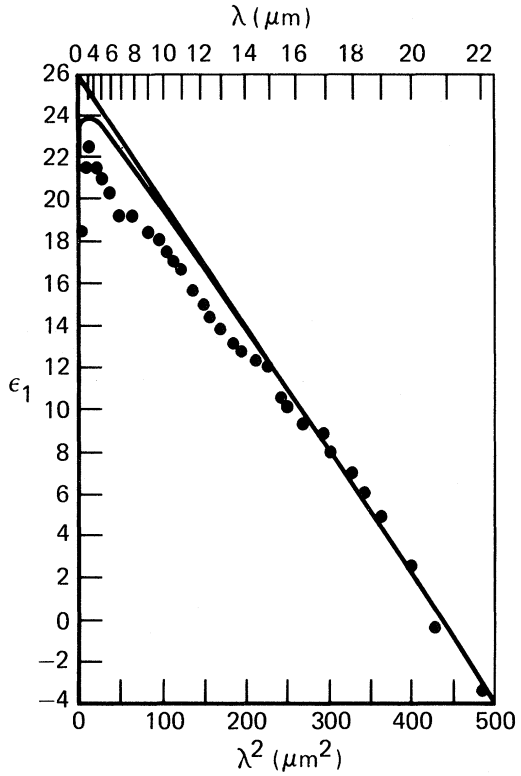

FIG. 9. The real part of the dielectric constant of α-Sn at 300 K. The upper curve is calculated with a wavelength-independent $\epsilon_1^{\text{inter}} = 26$. The lower curve is the infinite-lifetime RPA calculation of Sec. IV with $\epsilon_0 = 22.7$. The data points are from a 2.3×10^{18}-cm^{-3} p-type sample of Ref. 16.

Lindquist and Ewald[16] measured, with an ellipsometric technique, the real part of the dielectric function of α-Sn in the near infrared at room temperature. We have reanalyzed their data with the following results. As suggested in Ref. 6, the presence of thermally excited carriers at room temperature considerably modifies the wavelength dependence of $\epsilon_1^{\text{inter}} - \epsilon_0$ from a $\lambda^{1/2}$ behavior[15] in the region above 15 μm. Good fits can be obtained using the infinite-lifetime thermally broadened results of Sec. IV. In Fig. 9 is shown an example for a p-type sample with 2.3×10^{18} cm^{-3} acceptors. The upper curve is calculated with a frequency-independent $\epsilon_1^{\text{inter}} = 26$. The lower curve is calculated with the results of Sec. IV and yields a background dielectric constant of $\epsilon_0 = 22.7$. The fit in the region above 15 μm is extremely good, but not distinguishable from that with the wavelength-independent theory. Below 10 μm there is some disagreement from nonparabolic effects not included in the theory and probably phonon-assisted interband transitions, but it is interesting to note that the data display the same peaking behavior ($\lambda < 4$ μm) as the theory in all the samples. Fits for the other samples yield values of ϵ_0 ranging down to 18. The large scatter in the data may be due to lifetime-broadening effects which are probably important in heavily doped p-type samples. In any case, one could not expect to see the $\lambda^{1/2}$ dependence at room temperature in a reliable wavelength region, and thus a room-temperature experiment will yield very little information about the dielectric function.

Wagner and Ewald[22] measured the position of the reflectivity minimum at temperatures ranging from 250 to 26.1 K and at wavelengths as large as 218 μm. This is a region in which the temperature and wavelength dependences of $\epsilon^{\text{inter}}(\omega)$ become very important. Wagner and Ewald point out that, for lightly doped n-type α-Sn in the two-band region below about 120 K, the quantity $\lambda_0^2 T^{3/2}$, where λ_0 is the wavelength of the reflectance minimum, should be approximately constant. Yet their data show a temperature dependence, and they are unable to account for either the temperature variation or the large values of $\lambda_0^2 T^{3/2}$ by fitting with a temperature- and wavelength-independent $\epsilon_1^{\text{inter}}$ (see Figs. 6, 8, and 9 of Ref. 22).

Wagner and Ewald's analysis indicates that $\omega_0 \tau$ is very large, and thus we use the infinite-lifetime calculation of Sec. IV and assume that $\epsilon_2^{\text{intra}}$ of Eq. (7) is small enough to be ignored. We use the parameters of Wagner and Ewald: $\mu_c = \mu_c^* = 0.024$, $\mu_v = \mu_v^* = 0.24$, $\mu_1 = 0.19$, $\mu_1^* = 0.08$, $E_{g1}(0) = 0.11$ eV, and $\beta = 4 \times 10^{-4}$ eV/K, where μ_1 and μ_1^* are, respectively, the density-of-states and optical effective-mass ratios of the L_6^+ electrons, $E_{g1}(0)$ is the $L_6^+ - \Gamma_8^+$ gap at 0 K, and β is defined by

$$E_{g1}(T) = E_{g1}(0) - \beta T \ . \tag{60}$$

We calculate the wavelength λ_0 of the minimum

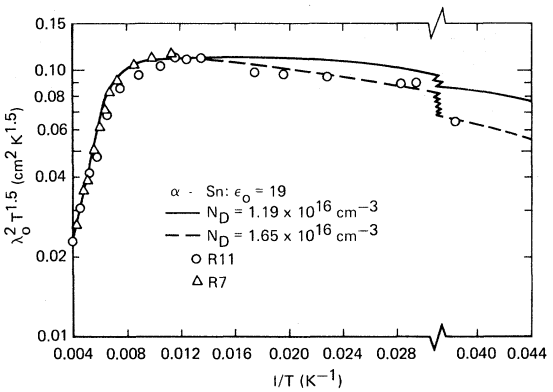

FIG. 10. The temperature dependence of the wavelength of the reflectivity minimum of α-Sn for donor concentrations corresponding to $n_e = 1.384 \times 10^{16}$ cm^{-3} at 26.1 K (solid curve) and to $n_e = 1.743 \times 10^{16}$ cm^{-3} at 26.1 K (dashed curve), with $\epsilon_0 = 19$ for both curves. The experimental data are from Ref. 22.

of the normal-incidence reflectivity,

$$R=\frac{(n-1)^2+k^2}{(n+1)^2+k^2} \quad , \tag{61}$$

where n and k are the real and imaginary parts of the index of refraction, respectively:

$$n=[\epsilon_1+(\epsilon_1^2+\epsilon_2^2)^{1/2}]^{1/2}/\sqrt{2}\,, \tag{62}$$

$$k=-\epsilon_2/2n\,. \tag{63}$$

For ϵ_0 we use a value of 19 which is near the mean of the values obtained from Lindquist and Ewald's data.[16] Wagner and Ewald's analysis of Hall data for sample $R11$ indicates an electron concentration of 1.384×10^{16} cm^{-3} at 26.1 K. This corresponds to a donor concentration of 1.19×10^{16} cm^{-3}. No value is given for the electron concentration of sample $R6$, except that it is in the low 10^{16}-cm^{-3} range. This makes very little difference in the analysis since the data for this sample only extend down to about 90 K, a range in which λ_0 is insensitive to donor concentration. The results of this calculation of $\lambda_0^2T^{3/2}$ vs $1/T$ for $N_D=1.19\times10^{16}$ cm^{-3} are given by the solid curve of Fig. 10. The data are in almost perfect agreement with the theory in the range 250–77 K. Between 77 and 30 K there is a small systematic discrepancy of about 10%. The lowest-temperature datum point, at 26.1 K and $\lambda_0=218$ μm, is in poor agreement. The value of ϵ_0 necessary to account for this point is 10.5. However, the value $\epsilon_0=10.5$ produces very large (30–40%) disagreements with the data at all other temperatures.

A possible explanation of the disagreement of the theory with the 26.1-K datum can be given as follows. It is very difficult to prepare α-Sn with a high homogeneity of impurities. Inhomogeneity can cause errors in the electron concentrations determined by Hall measurements. On the other hand, $\lambda_0^2T^{3/2}$ is extremely sensitive to donor concentration in this range of doping and temperature. If we assume that the Hall analysis underestimates the electron concentration by about 20% at 26.1 K, that is, that there are 1.743×10^{16}-cm^{-3} electrons at 26.1 K corresponding to a donor concentration of 1.65×10^{16} cm^{-3}, then the calculation yields the dashed curve in Fig. 10. The theory is now in excellent agreement with experiment at 26.1 K. Above 77 K the theory is insensitive to N_D and the calculations for the two values of N_D are negligibly different. Between 77 and 30 K, even the small systematic discrepancy has been removed.

Other possibilities are that the RPA is highly inaccurate, about which we have no comment, or that ϵ_0 does suddenly change by a factor of 2 between 35 and 25 K. The latter would be highly unusual, although one cannot rule out some anomaly in the lattice polarizability.

We feel that this experiment provides strong support for the temperature and wavelength dependences of the dielectric function predicted by the RPA. Only very poor fits to these data can be obtained using a temperature- and frequency-independent $\epsilon_1^{\text{inter}}$. The reason for this is clear from Fig. 11, where the real part of the RPA interband dielectric function, evaluated at the wavelength of the reflectivity minimum, is displayed as a function of $1/T$. These values do give good agreement with experiment, and the variation with temperature is quite large. Thus, it is difficult to see how any temperature- and wavelength-independent $\epsilon_1^{\text{inter}}$ could also give agreement over this temperature range.

It would be extremely important to carry this experiment to lower temperatures with a large range of donor concentration, and with electrical measurements at liquid-helium temperatures where Hall and Shubnikov-de Haas measurements of n_e could be compared for consistency.

One would be inclined to dismiss the point at 26.1 K with the above explanation, were it not for the effect that the value of ϵ_0 obtained from it has on the mobility calculation for α-Sn. Figure 12 shows the ionized-impurity-limited mobility as a function of donor concentration, using the theory of Ref. 11 as amended by Refs. 13 and 14. The dotted curve is the RPA calculation for $\epsilon_0=19$. It is in somewhat better agreement with experiment than the previous calculation[11,13,14] using $\epsilon_0=24$, but still lies about twice as high as the data. The solid curve is this calculation superimposed on a neutral scattering mechanism[14] with a mean-free path of about 2.3 μm. The results are about the same as those of Refs. 13 and 14, except that the agreement with experiment is somewhat better in

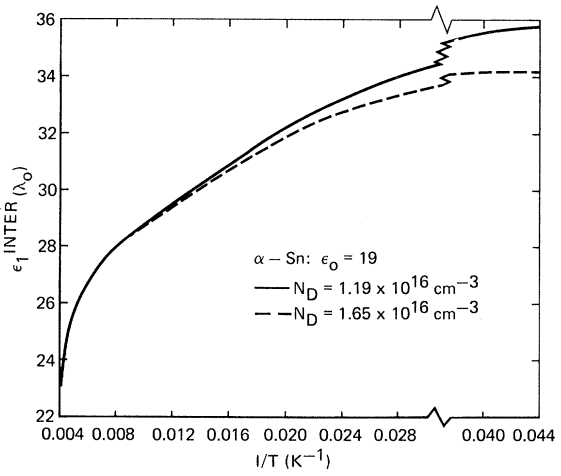

FIG. 11. The real part of the interband dielectric function evaluated at the reflectivity minimum as a function of $1/T$ for two donor concentrations.

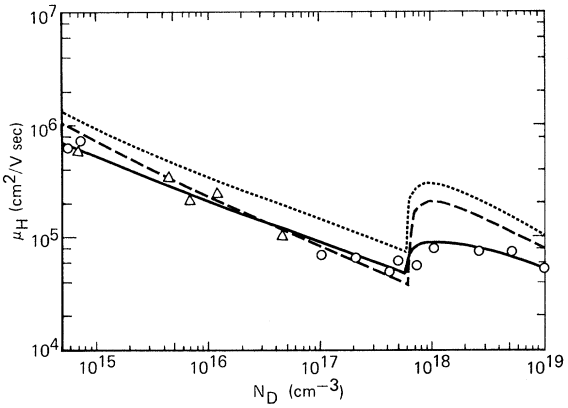

FIG. 12. Ionized-impurity-limited mobility of the Γ_8^+ electrons of degenerate n-type α-Sn as a function of donor concentration. The dotted curve is the RPA calculation of Ref. 11, 13, and 14 with $\epsilon_0 = 19$. The solid curve is the dotted curve superimposed on the neutral scattering mechanism of Ref. 14 with an electron-concentration-independent mean-free path of ~ 2.3 μm. The dashed curve is the RPA calculation of Ref. 11, 13, and 14 with $\epsilon_0 = 10.5$.

the 10^{17}-cm^{-3} region, and the density of neutral 5-Å scatterers is reduced to about 1.5×10^{18} cm^{-3}. The dashed curve is the RPA-screened ionized-impurity-limited mobility calculation for $\epsilon_0 = 10.5$. It is 20–35% higher than the data in the 10^{14}-cm^{-3} region, which could easily be accounted for by a small amount of compensation. However, in the range $N_D = 10^{15} - 5\times10^{17}$ cm^{-3} it is in very good agreement with experiment. Above $N_D = 5\times10^{17}$ it is grossly in error. However, it must be remembered that in this region of two-band conduction, the screening by the L_6^+ electrons, which produces the large enhancement of Γ_8^+ electron mobility, has been calculated in the Fermi-Thomas approximation. Because of the ellipsoidal shape of the L_6^+ Fermi surface and the angular dependence of the L_6^+ overlap matrix element, the Fermi-Thomas approximation may be quite inaccurate. We have recently analyzed[13] an analogous situation for screening by the Γ_8^+ electrons, where there are large screening losses at high momentum transfer ($q \sim 2k_F$). In that case the mobility is only slightly affected because the intraband screening is dominated by the interband screening at $q \sim 2k_F$. However, this may not be true for the high-mass L_6^+ electrons, especially with an ϵ_0 as low as 10.5. This calculation is being pursued.

It should be noted that ϵ_0 of this theory should not be identified with ϵ_{00}, the homopolar static dielectric constant of the Phillips[28] and Van Vechten[29] theory. The relation between these quantities is unclear for two reasons. First, it is not clear what states contribute to ϵ_{00} in a structure with a divergent interband static dielectric constant. Second, the separation of $\epsilon_1^{\text{inter}}$ into contributions from the "Γ_8 bands" and "all other bands" is purely arbitrary so long as it is made at an interband energy above which the terms in the sum are nearly independent of frequency and carrier concentration (in the range of interest) and below which they are accurately given in the parabolic approximation. A suitable energy for such a cutoff of the Γ_8 contribution would be around 0.4 eV in our case (see Ref. 11 for a discussion of the parabolic approximation). For convenience and because of its arbitrariness, we have in fact made no cutoff; i.e., we have extended the parabolic bands to infinity. The resulting small contribution to the Γ_8 part is independent of frequency and carrier concentration in the range of interest and is thus absorbed into ϵ_0 in the fitting procedure. Thus, although this procedure yields accurate values of the total $\epsilon_1^{\text{inter}}$ and is in fact the same as that used in the mobility calculation,[7–14] only the total $\epsilon_1^{\text{inter}}$ has unambiguous physical meaning.

Another point worth mentioning concerns the temperature dependence of E_{g1}. Other values of E_{g1}, μ_1^*, and β were tried, but none yielded a fit nearly so good in the three-band region as that shown in Fig. 10, with $E_{g1}(0) = 0.11$ eV, $\beta = 4\times10^{-4}$ eV/K, and $\mu_1^* = 0.08$. For these values, L_6^+ crosses Γ_8^+ at 275 K, a value remarkably close to the temperature of transition to the β phase[30] (286 K). It is interesting to speculate whether this crossing, or the fact that the indirect exciton energy at this temperature would then be lower than Γ_8^+, is connected with the phase transition.

VII. SUMMARY

We have analyzed the temperature, wavelength, and impurity-concentration dependences of the long-wavelength RPA dielectric function of α-Sn. At absolute zero, $\epsilon_1^{\text{inter}}(\omega)$ is divergent at $\hbar\omega = (1+\gamma)E_F'$. Although temperature and lifetime broadening remove the divergence, the effect should still be experimentally observable at liquid-helium temperatures. Similar considerations also apply to HgSe and HgTe. The nondegenerate limit and cases of intermediate degeneracy have also been analyzed. Strong supporting evidence is found for the temperature and wavelength dependences predicted by the RPA in the reflectivity minimum experiment of Wagner and Ewald. More experimental work is needed to establish the value of ϵ_0 with certainty. Theoretical work on the effect of these unusual properties of the dielectric function on the lattice dynamics of the symmetry-induced zero-gap structures should also be profitable.

ACKNOWLEDGMENTS

I am grateful to Dr. C. R. Whitsett, Dr. S. L.

Lehoczky, and Dr. S. Zwerdling for useful discussions of this problem. I would also like to thank Dr. R. J. Wagner for very helpful discussions of his and Professor Ewald's experiment, and Dr. J. C. Phillips for a most informative discussion of the ionicity theory.

*Research conducted under the McDonnell Douglas Independent Research and Development Program.

[1]S. Groves and W. Paul, Phys. Rev. Letters 11, 194 (1963).

[2]L. Liu and D. Brust, Phys. Rev. Letters 20, 651 (1968).

[3]L. Liu and D. Brust, Phys. Rev. 173, 777 (1968).

[4]D. Sherrington and W. Kohn, Rev. Mod. Phys. 40, 767 (1968).

[5]B. I. Halperin and T. M. Rice, Rev. Mod. Phys. 40, 755 (1968).

[6]J. G. Broerman, Phys. Rev. Letters 25, 1658 (1970).

[7]L. Liu and E. Tosatti, Phys. Rev. Letters 23, 772 (1969).

[8]J. G. Broerman, Phys. Rev. 183, 754 (1969).

[9]J. G. Broerman, Phys. Rev. Letters 24, 450 (1970).

[10]L. Liu and E. Tosatti, Phys. Rev. B 2, 1926 (1970).

[11]J. G. Broerman, Phys. Rev. B 1, 4568 (1970).

[12]J. G. Broerman, Phys. Rev. B 2, 1818 (1970).

[13]J. G. Broerman, L. Liu, and K. N. Pathak, Phys. Rev. B 4, 664 (1971).

[14]J. G. Broerman, J. Phys. Chem. Solids 32, 1263 (1971).

[15]D. Sherrington and W. Kohn, Phys. Rev. Letters 21, 153 (1968).

[16]R. E. Lindquist and A. W. Ewald, Phys. Rev. 135, A191 (1964).

[17]E. D. Hinkley and A. W. Ewald, Phys. Rev. 134, A1260 (1964).

[18]C. F. Lavine and A. W. Ewald, J. Phys. Chem. Solids 32, 1121 (1971).

[19]C. R. Whitsett, Phys. Rev. 138, A829 (1965).

[20]R. R. Galazka, D. G. Seiler, and W. M. Becker, in Proceedings of the Conference on Semimetals and Narrow Gap Semiconductors, Dallas, 1970 (unpublished).

[21]V. I. Ivanov-Omskii, B. T. Kolomietz, V. K. Ogorodnikov, and K. P. Smekalova, Fiz. Tekh. Poluprov. 4, 264 (1970) [Sov. Phys. Semicond. 4, 214 (1970)].

[22]R. J. Wagner and A. W. Ewald, J. Phys. Chem. Solids 32, 697 (1971).

[23]H. Ehrenreich and M. H. Cohen, Phys. Rev. 115, 786 (1959).

[24]P. Nozières and D. Pines, Nuovo Cimento 9, 470 (1958).

[25]P. Nozières and D. Pines, Phys. Rev. 109, 762 (1958).

[26]J. McDougall and E. C. Stoner, Phil. Trans. Roy. Soc. London A237, 350 (1938).

[27]B. L. Booth and A. W. Ewald, Phys. Rev. 168, 805 (1968).

[28]J. C. Phillips, Phys. Rev. Letters 20, 550 (1968).

[29]J. A. Van Vechten, Phys. Rev. 182, 891 (1969).

[30]E. Cohen and A. K. W. A. van Lieschert, Z. Physik. Chem. Leipzig 173, 1 (1935); 173, 32 (1935); 173, 67 (1935).

PHYSICAL REVIEW B VOLUME 5, NUMBER 2 15 JANUARY 1972

Concentration and Temperature Dependence of Impurity-to-Band Activation Energies

G. F. Neumark
Philips Laboratories, Briarcliff Manor, New York 10510
(Received 2 March 1971)

The present paper investigates the cause of the experimentally well-known reduction of impurity activation (ionization) energies in the intermediate doping range. It is shown that this many-body problem can be reasonably approximated by a one-electron screened-impurity approach. Application of this result to literature data on GaP(Zn) gives agreement with the experimental results provided that screening by ionized impurities is included; screening by free carriers alone is insufficient. The inclusion of the ionized impurity screening thus for the first time provides a *quantitative* explanation for the observed reductions in activation energies. A corollary of the screening effect is that the activation energy decreases with increasing temperature; use of this temperature dependence clarifies previous discrepancies between Hall and neutron activation values for the Zn concentration in GaP.

I. INTRODUCTION

It has been known since the work of Pearson and Bardeen[1] in 1949 that impurity activation energies decrease at high impurity concentrations, i.e., the average separation between the impurity levels and the band decreases with increasing impurity concentration. In the present paper, we shall consider only the case of "intermediate" doping, where this separation has not decreased too far, i.e., the impurity band has not yet appreciably merged with the conduction band.[2] (The high doping range is already reasonably well understood.[2,3]) In the intermediate range, it has been shown by Fritzsche[4] that, in